Role of Water in Transient Cytochrome c_2 Docking

Felix Autenrieth,[†] Emad Tajkhorshid,[‡] Klaus Schulten,[‡] and Zaida Luthey-Schulten*[,†,‡]

Department of Chemistry and Beckman Institute, University of Illinois at Urbana−Champaign, Urbana, Illinois 61801

Received: May 10, 2004; In Final Form: August 25, 2004

Cytochrome *c* (cyt *c*) is a small water-soluble redox protein that facilitates electron transfer in photosynthesis and respiration by alternately docking to integral membrane proteins such as the photosynthetic reaction center (RC). Recently, a high-resolution X-ray structure was solved for the RC−cyt c_2 complex of *Rhodobacter sphaeroides*, revealing important contacts between the RC in its ground state and reduced cyt c_2 mediated by bridging water molecules. In this article, we compare the variations in these contacts and in the interface in general for both redox states of cyt c_2 that resulted from full-atom simulations of the complexes embedded in a membrane with explicit water molecules. Molecular dynamics simulations of the two redox states of the RC−cyt c_2 system were performed using the CHARMM27 parameters developed for the oxidized and reduced forms of the heme prosthethic group. In its overall dynamics, the encounter complex was found to be very similar in both redox states, exhibiting at the interface a stable hydrophobic tunneling domain and a broad basin of attraction. The differences between the redox states are subtle and involve the formation of a structured cluster of water molecules in the reduced cyt c_2 system. Fluctuations of water and residues at the interface increase upon oxidation and probably mediate the undocking process. The observed differences between the two redox states of the system can only be attributed to the different electrostatic potentials generated by heme in the interface region, as no other modifications were introduced. As the time scale of the undocking process is beyond the time scales reachable by full atomic molecular dynamics simulation of the system, we employed steered molecular dynamics to investigate and compare the energetics associated with the unbinding of RC−cyt c_2 in the reduced and oxidized forms.

1. Introduction

Cytochrome *c* (cyt *c*) is a small water-soluble redox protein that facilitates electron transfer in photosynthesis and respiration by alternately docking to integral membrane proteins. Cyt *c* is the best studied electron transport protein in terms of structure and interaction with membrane protein complexes.[1,3] In the photosynthetic apparatus of purple bacteria cyt c_2 shuttles electrons between the bc_1 complex and the reaction center (RC).[4] In moving back and forth between these two membrane protein complexes, cyt c_2 is reduced upon docking to the bc_1 complex and oxidized upon docking to the RC, effectively transferring one electron from the bc_1 complex to the RC. In cyclic photosynthesis, the main energy source of purple bacteria, electronic charge separation, is performed in the RC and the resulting electron hole filled up by reduced cyt c_2. Light energy generates a proton gradient across the photosynthetic membrane through the bc_1 complex and RC system; the proton gradient drives then the synthesis of ATP by ATPase.

Until recently only rather uncertain models of the RC−cyt c_2 complex were available. The models exploited the structural arrangement of photosynthetic pigments in RCs containing a nondissociating cytochrome[5−7] as can be found in the high-resolution X-ray structure of *Blastochloris viridis*.[8] In 2002, a high-resolution X-ray structure was solved for the RC−cyt c_2 cocrystal of *Rhodobacter (Rb.) sphaeroides*,[1] in which cyt c_2 is in the reduced state and RC is in the ground state. The structure exhibits many features predicted by the earlier models. For example, the docking interface can be divided into a short-range hydrophobic and hydrogen bonding docking domain surrounded by a long-range electrostatic docking domain with complementary charged residues on the RC and cyt c_2.[1,9] Interestingly, in the X-ray structure none of these charged residues forms a direct salt bridge as proposed earlier.[5,6] The presence of only weak protein−protein interactions in the crystal structure supports a transient formation of the RC−cyt c_2 complex. The docking of the RC and cyt c_2 is highly dependent on a ring of conserved lysines around the heme crevice and on clusters of negatively charged residues on the RC surface.[9,10] Positively charged residues on cyt c_2 that are important for electrostatic steering are structurally conserved in all three domains of life.[7,11,12] Tetreault et al. have determined the importance of each of these charged residues for cyt c_2 docking by point mutation of negatively charged residues on the RC[9] as well as double mutations of the RC−cyt c_2 complex with a homologous cyt c_2 from *Rhodobacter capsulatus*.[10] Reduced cyt c_2 with the heme iron in the Fe^{2+} state (cyt c_2^{red}) can transfer an electron to the charge separated RC ($RC(P^+Q_A^-)$) and thereby, convert to oxidized cyt c_2 with the heme iron in the Fe^{3+} state (cyt c_2^{ox}):

$$\text{Cyt } c_2^{red}\text{:RC(PQ}_A\text{)} \xrightarrow{h\nu} \text{Cyt } c_2^{red}\text{:RC(P}^+\text{Q}_A^-\text{)} \xrightarrow{k_e} \text{Cyt } c_2^{ox}\text{:RC(PQ}_A^-\text{)} \quad (1)$$

In experimental studies of electron transfer,[1] binding of cyt c_2^{red} to ground-state RC ($RC(PQ_A)$) reaches an equilibrium resulting

* Corresponding author. E-mail: zan@uiuc.edu. Mailing address: 600 South Mathews Ave., Urbana, IL 61801. Telephone: (217) 333-3518. Fax: (217) 244-3186. Web: http://www.scs.uiuc.edu/∼schulten.
† Department of Chemistry, University of Illinois at Urbana−Champaign.
‡ Beckman Institute, University of Illinois at Urbana−Champaign.

10.1021/jp047994q CCC: $27.50
Published on Web 12/01/2004

in the presence of both free and bound cyt c_2^{red} in the sample before excitation. After application of a laser flash both fast and slow electron-transfer kinetics were observed. The fast phase is due to cyt c_2 already bound to RC(PQ_A) before the flash, and the slow phase corresponds to the association of free cyt c_2 to RC($P^+Q_A^-$). The prosthetic groups involved in the electron-transfer reaction are one heme in cyt c_2 and two bacteriochlorophylls, termed the special pair, in RC.[13] The special pair can exist in the ground state (*P*) or in the charge separated state (P^+). After charge separation an electron is transferred from the special pair to a tightly bound ubiquinone (Q_A) inside the RC, creating an electron hole in the special pair that is filled up eventually by oxidation of cyt c_2.

It is known from experimental[14−17] and theoretical studies[18] that dominant electron transfer pathways from cyt c_2 to the RC are established over conserved residues, such as TyrL162 at the contact interface (here TyrL162 denotes Tyr residue 162 of the L subunit). The dominant electron pathways provide a means for a fast, first order electron transfer with a half-time in the microseconds range. The replacement of TyrL162, LeuM191, or ValM192 by Ala decreases the electron transfer rate constant k_e by factors of 120, 9, and 0.6, respectively.[17] It is also feasible to establish dominant electron-transfer pathways over single bound water molecules.[18] Stable electron-transfer pathways between donor and acceptor are necessary for effective tunneling.[16]

The most effective electron transfer pathways in proteins include electron jumps over sigma and hydrogen bonds from the donor to the acceptor site. Large jumps through space can decrease the rate by several orders of magnitude. Electron transfer in proteins is therefore highly modulated by the structure of the protein surrounding the donor and acceptor sites. These hardwired electron pathways are very often comprised of conserved amino acid residues in both intra- and interprotein electron-transfer reactions.[16,19]

The special problem of association and dissociation arises in interprotein electron transfer of transient complexes. In electron-transfer complexes the docking interfaces of cyt *c* with cyt *c* peroxidase,[20] the bc_1 complex[3] as well as the RC[1] tend to be very small (<1200 Å^2) as the complexes form dynamically. It is necessary on the one hand that transient electron transfer complexes are bound tightly enough to ensure optimal tunneling rates, but on the other hand they should be loose enough to dissociate readily after electron transfer has occurred. Mutational studies on the RC−cyt c_2 complex of *Rb. sphaeroides* indicate that the first-order electron-transfer rate constant k_e and the association constant k_A are correlated. This finding suggests that the key residues for electron transfer, TyrL162, LeuM191, and ValM192, establish electron-transfer pathways by well-defined van der Waals (VDW) contacts.[17] Kinetic studies of horse heart cyt *c* bound to the *Rb. sphaeroides* photosynthetic RC indicate that cyt *c* binds more tightly after oxidation[21] while different redox states of native cyt c_2 have comparable binding affinities.[44] These observations suggest that there may be a cyt c_2^{ox} specific mechanism by which the protein can undock more readily than does cyt c_2^{red}. In cyclic photosynthesis it is functionally very important that cyt c_2^{ox} undocks in order to make space for another reduced cyt c_2^{red}, which needs to dock for the next round of electron transfer to the RC.

In this paper we report molecular dynamics (MD) simulations of the RC−cyt c_2 encounter complex[1] for both redox states of cyt c_2. As shown in Figure 1, the RC−cyt c_2 complex was embedded in a lipid bilayer and equilibrated without any constraints for 4 ns. Cyt c_2 was pulled by means of steered molecular dynamics (SMD)[22−24] 10 Å away from the RC starting from the equilibrated structure. Simulations with cyt c_2^{red} and cyt c_2^{ox} were performed using CHARMM27 parameters for the heme prosthetic group furnished in ref 2. The simulations revealed that water molecules at the RC−cyt c_2 interface exhibit higher mobility in cyt c_2^{ox}. A clearly different water structure can be observed in a hydrophobic binding pocket close to the TyrL162/Heme edge contact region, which has been shown by experimental and theoretical studies[14,15,18] to be of major importance for electron transfer across the RC−cyt c_2 interface. We suggest that the change in water structure in this hydrophobic pocket is of central importance for undocking after oxidation.

To complement a recent paper on the electrostatic contribution to the binding,[25] we also determined the VDW and electrostatic interaction energies during the course of equilibration and SMD. During equilibration and the initial phase of undocking, the RC−cyt c_2 complex is stabilized primarily by VDW interactions with the long-range electrostatic energy playing an increasingly important role as the complex is pulled apart. Together with the data obtained from mutational studies[9,10] our results suggests that the VDW energy is of major importance for the docked RC−cyt c_2 complex. To estimate the range of motion of cyt c_2 at the docking interface we have evaluated the VDW interaction for cyt c_2 docked at various positions along the RC surface.

2. Computational Methods

2.1. System Setup. The recently solved 2.4 Å X-ray structure of the RC−cyt c_2 complex from *Rb. sphaeroides*[1] was used as the starting point for all simulations. The original coordinate system of the RC−cyt c_2 complex was transformed to orient the L and M subunits of the RC along the *z*-axis. The pseudo-2-fold symmetry of these two subunits was therefore exploited and the symmetry axis pointing directly through the non-heme iron orthogonal to the cytoplasmic and periplasmic space was used. Structurally not resolved residues of the H subunit (1−7 and 254−256) and of the M subunit (302−307) were added with the program Modeler in InsightII[26] using as template the high-resolution RC structure by Stowell et al.[27] The coordinates of the missing ubiquinone Q_B and the carotenoid spheroidene were obtained from the RC structure with PDB accession code 1YST.[28] The RC−cyt c_2 X-ray structure from Axelrod et al.[1] was obtained from RCs of the carotenoidless mutant of *Rb. sphaeroides* strain R26 with PDB accession code 1L9B. BChla-histidine patches and non-heme iron RC patches were used in a protocol similar to the one described in ref 29. The simulations were setup employing the program PSFGEN through VMD[30] with the CHARMM27 force field.[31,32] All titratable residues were modeled in their charged states.

Using the CHARMM27 parameters reported for the cyt *c* heme prosthetic group in ref 2, complete systems for the cyt c_2^{red} and cyt c_2^{ox} were generated. These systems contain charge neutral special pairs and resemble closely the reduced and oxidized encounter complexes employed for kinetic studies before application of the laser flash.[1,9]

All detergent molecules present in the structure PDB 1L9B were removed and the protein was placed in a POPC lipid bilayer. All resolved crystallographic water molecules were included in both RC−cyt c_2 complexes for simulation. After addition of unspecified hydrogens to the structures PDB 1YST and 1L9B, the complexes were solvated with explicit TIP3 water molecules[33] using the SOLVATE feature of VMD.[30,34,35] Additional layers of water molecules were added on the periplasmic side of the systems in order to allow pulling of cyt c_2 for up to

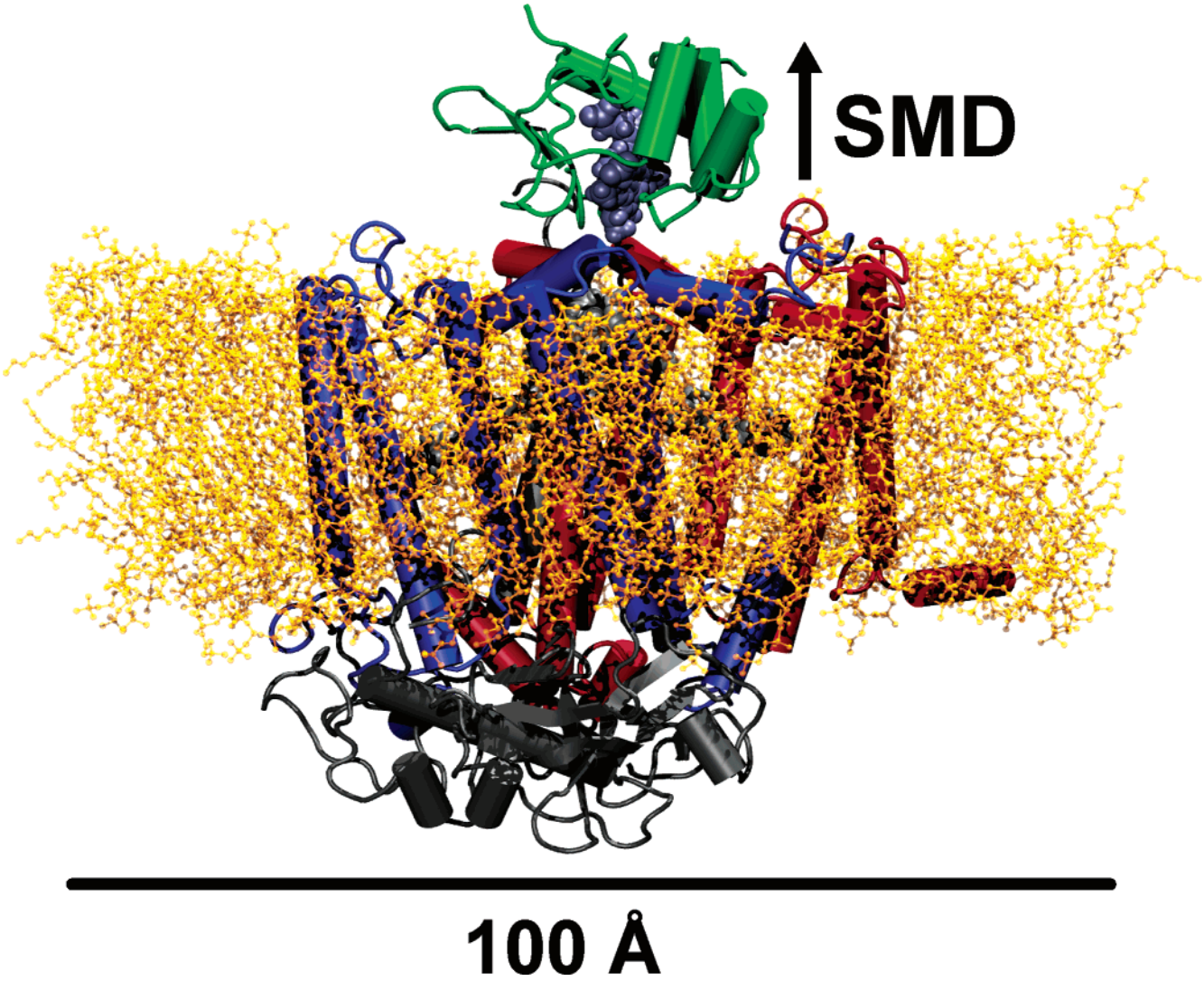

Figure 1. Simulated RC−cyt c_2 complex of *Rb. sphaeroides*. The transmembrane parts of the L (blue), M (red), and H (gray) subunits of RC are embedded in a lipid bilayer (orange). The complex was equilibrated for 4 ns. Cyt c_2 is shown after equilibration for 4 ns (green). The black arrow indicates the 10 Å pulling of cyt c_2 away from the RC docking surface.

15 Å in a subsequent SMD simulation ensuring proper solvation in all stages. The initial water box was cut to a hexagonal prism of approximately 140 Å height. To ensure proper hydration of all internal cavities, the program DOWSER[36] and a potential energy cutoff of −15 kcal/mol were used. The results confirmed that all buried crystal water molecules are at energetically favorable positions.

Six additional water molecules were found by DOWSER in the H subunit, which is located at the cytoplasmic side of the RC and not part of the periplasmic docking interface. To neutralize the systems as needed for our electrostatics calculations described below five and four sodium ions were added to the reduced and oxidized systems, respectively. The final systems contained approximately 145 700 atoms, 15 480 of which belong to the complex. The simulated system is shown in Figure 1.

2.2. Molecular Dynamics Simulations. All MD simulations were carried out using the parallel molecular dynamics program NAMD2[34] and the CHARMM27 force field for lipids and proteins.[31,32] The newly developed parameters for the heme prosthetic group[2] and the photosynthetic pigments[29] were used.

Equilibrations were performed in the NPT ensemble with a cutoff of 12 Å (switching function starting at 10 Å) for VDW interactions. Periodic boundary conditions applied with a flexible cell. Distances between periodic images of the protein were greater than 15 Å in all cases. The particle mesh Ewald (PME) method[37] was employed for computation of electrostatic forces; a cutoff of 12 Å was used for computing the direct sum of the forces. An integration time step of 1 fs was assumed, permitting a multiple time-stepping algorithm[38] to be employed in which interactions involving covalent bonds were updated every time step, short-range nonbonded interactions were updated every two time steps, and long-range electrostatic forces were updated every four time steps. In all simulations, Langevin dynamics was utilized to keep a constant temperature of 298 K; likewise, the hybrid Nosé−Hoover Langevin piston method was used to control a constant pressure of 1 atm.

The simulations proceeded initially as follows. First lipids and water molecules were equilibrated for 0.5 ns while keeping the RC−cyt c_2 complex fixed until the volume converged. Then a stepwise minimization of the RC−cyt c_2 complexes was carried out: first all water and lipid molecules as well as protein hydrogen atoms were minimized for 5000 steps, then protein side chains were minimized for 5000 steps, and finally the whole system was released and minimized for 10 000 steps. The final equilibrations of 4 ns were performed without any constraints. The RMSD of C_α atoms calculated with respect to the X-ray

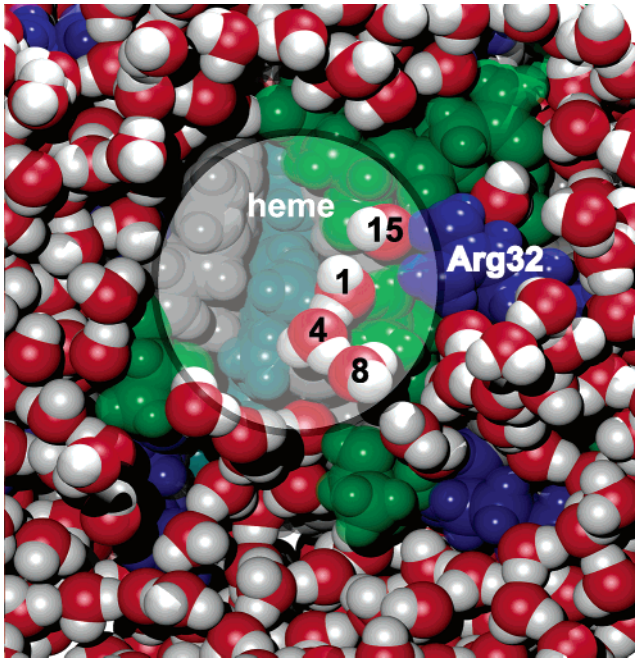

Figure 2. Top down view of the cyt c_2^{red} surface after 2 ns of equilibration. The hydrophobic docking domain (circle) is in direct contact or is separated by a single layer of water molecules from the RC above (omitted for clarity). The four water molecules (Wat15, Wat1, Wat4, Wat8) and ArgC32 form a stable single-file of hydrogen bonds. The surrounding electrostatic docking domain is highly solvated. Positively charged residues are depicted in blue, polar residues in green, hydrophobic residues in gray, and the exposed heme edge in cyan.

structure of the RC−cyt c_2 complex fluctuated around 2.4 Å during the last 0.5 ns of equilibration.

2.3. SMD Simulations. To simulate the undocking of cyt c_2 from the RC, external forces along the *z*-axis were applied to all backbone atoms of cyt c_2. The side chains and the heme group were allowed to move freely.

The external force F had the form:

$$F = k(vt - \Delta z) \tag{2}$$

In this form Δz is the displacement of the center of mass of the pulled atoms relative to its original position, v is the constant velocity of a spring attached to the center of mass of the pulled atoms,[39] and k is the spring constant. The SMD simulation was performed in the *NVT* ensemble with a spring constant k of 20 kcal/mol Å^2 (1388.7 pN/Å) and a pulling speed of 0.005 Å/ps. The time evolution of the force (F) and the *z*-displacement of the cyt c_2 center of mass were recorded every 0.1 ps. The chosen force constant corresponds to a thermal disorder in Δz (RMSD) of $\sqrt{k_B T/k} \approx 0.2$ Å, which is much smaller than the spatial resolution needed to monitor a 10 Å separation between RC and cyt c_2. During the simulations the RC moved by about 0.5 Å, which is small relative to the overall displacement of cyt c_2 during the forced undocking. Visualization and analyses of the simulations used the program VMD.[30]

2.4. Energy Landscape for Protein—Protein Docking. To investigate the energy landscape and the geometric fit of the encounter complex between cyt c_2 and the RC at the proposed docking site, cyt c_2 was translated along the RC surface without water present. For this purpose, cyt c_2 was moved in 1-Å steps 4 Å in each direction. At each point the structure of the complex was minimized for 20 000 steps in NAMD2[34] and the VDW interaction energy between cyt c_2 and the RC calculated as a measure of the geometric fit. The origin was set at the position

TABLE 1: Distances (Å) Measured between RC and cyt c_2 Residues from X-ray Structure and Averages Taken from the Last 2 ns of Equilibration for Both Redox States

RC atom	cyt c_2 atom	X-ray [1]	mean red.	std red.	mean ox.	std ox.
		Electrostatic				
AspL155:$O_{\delta1}$	ArgC32:$N_{\eta1}$	7.0	8.6	0.7	8.7	1.4
AspL257:$O_{\delta2}$	LysC99:N_ζ	5.3	5.1	1.2	5.6	0.9
AspL261:$O_{\delta1}$	LysC97:N_ζ	5.3	4.0	1.3	3.9	0.6
AspL261:$O_{\delta2}$	LysC99:N_ζ	4.8	5.5	1.1	10.0	1.0
GluM95:$O_{\epsilon2}$	LysC103:N_ζ	8.0	7.5	1.0	9.3	1.0
GluM95:$O_{\epsilon1}$	LysC103:N_ζ	8.6	8.0	1.0	9.1	1.4
GluM173:$O_{\epsilon2}$	LysC105:N_ζ	9.0	9.9	1.3	5.2	0.8
GluM173:$O_{\epsilon2}$	LysC106:N_ζ	5.3	9.0	1.1	11.2	1.4
AspM184:$O_{\delta1}$	LysC97:N_ζ	8.1	13.1	2.5	13.9	1.2
AspM184:$O_{\delta2}$	LysC103:N_ζ	6.9	7.5	1.0	6.6	1.3
AspM292:$O_{\delta2}$	LysC106:N_ζ	8.5	14.6	1.5	14.3	1.9
AspM292:$O_{\delta2}$	LysC10:N_ζ	5.7	8.4	1.1	7.8	2.0
		VDW				
TyrL162:$C_{\delta1}$	heme:CBC	4.0	3.9	0.2	4.0	0.2
TyrL162:$C_{\epsilon1}$	heme:CBC	4.0	4.1	0.2	4.1	0.3
TyrL162:C_β	ThrC36:O1	3.7	3.8	0.4	3.8	0.4
GlyL165:C_α	ThrC101:$C_{\gamma2}$	3.8	4.0	0.3	4.4	0.4
AsnM188:$O_{\delta1}$	PheC102:$C_{\delta1}$	3.5	4.0	0.6	5.1	1.0
LeuM191:O	GlnC14:C_β	3.4	4.3	0.4	4.0	0.4
LeuM191:$C_{\delta1}$	ThrC17:$C_{\gamma2}$	3.6	4.2	0.4	4.3	0.5
LeuM191:C_β	PheC102:$C_{\delta1}$	3.5	4.3	0.4	3.7	0.2
LeuM191:C_γ	heme:CMC	3.9	4.6	0.3	4.8	0.3
ValM192:C_α	GlnC14:$O_{\epsilon1}$	3.8	5.1	0.6	4.8	0.5
ValM192:$C_{\gamma2}$	PheC102:$C_{\epsilon1}$	3.6	4.7	0.5	4.9	0.5
AsnM293:$N_{\delta2}$	AsnC13:C_β	3.3	4.0	0.4	3.8	0.3
ValM296:$C_{\gamma2}$	AsnC13:$N_{\delta2}$	3.9	6.1	0.8	4.3	0.5
		Hydrogen Bond				
GlnL258:$N_{\epsilon2}$	LysC99:O	3.3	3.2	0.4	3.3	0.4
AsnM187:$N_{\delta2}$	ThrC101:O	3.0	5.1	0.7	4.6	0.9
AsnM188:$O_{\delta1}$	LysC103:N	3.1	5.6	0.3	6.4	0.9
		Cation−π				
TyrM295:$C_{\delta2}$	ArgC32:N_ϵ	3.4	3.8	0.3	4.1	0.5

derived from the reduced or oxidized minimized RC−cyt c_2 complexes, respectively. The VDW energy will be referred to as the docking energy between cyt c_2 and RC and can be used to determine the best fit between cyt c_2 and RC. The same set of CHARMM27 force field parameters[2,31,32] as for the MD and SMD simulations was employed. The cutoff in the VDW scan was 12 Å.

The VDW and electrostatic energy contributions over the whole 4 ns equilibration as well as the SMD trajectories were monitored using the program MDforce in the NAMD2 package.[34] MDforce extracts positions and velocities of specified atoms from the trajectory file and evaluates the interaction energies according to the CHARMM energy function. The electrostatic and VDW interaction energy contributions between RC and cyt c_2 were obtained from the trajectories and are shown in Figure 10. A dielectric constant of 1 was assumed. The electrostatic energies originally obtained by setting the dielectric constant to 1 were later rescaled by a factor of 10 as shown in Figure 10 to approximate the dielectric effects of interface water. There are no cutoff factors for either energy term employed for the MDforce calculations.

3. Results and Discussion

Below we discuss the dynamic docking interface and the variations in the VDW and electrostatic interactions upon the undocking of cyt c_2.

3.1. The Dynamic Docking Interface. Figure 2 shows a snapshot of the cyt c_2^{red} docking surface after 2 ns of equilibration. The dynamics of the interface can be understood best by

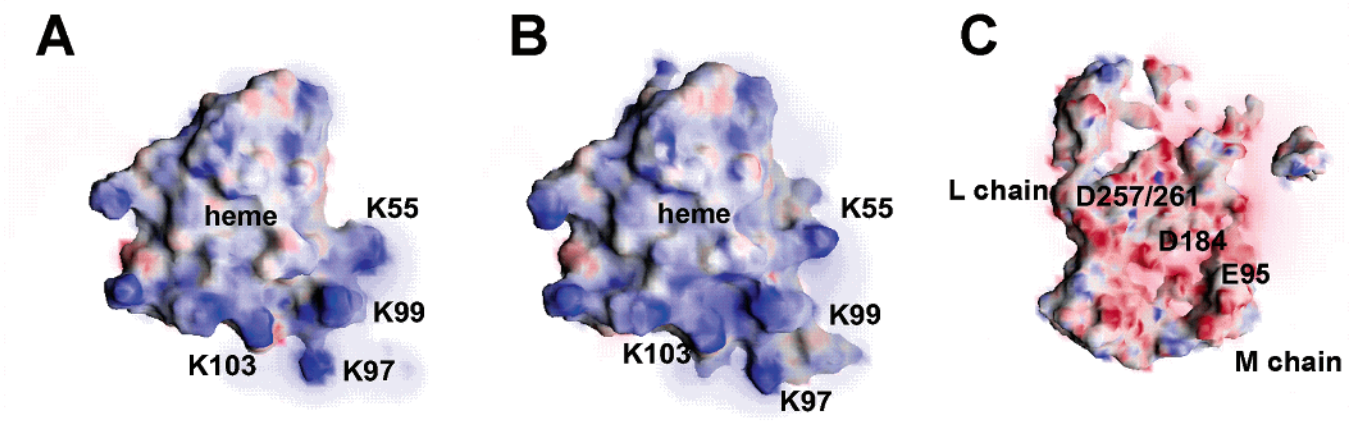

Figure 3. DelPhi generated electrostatic potential at the docking surface of cyt c_2 in its reduced (A) and oxidized (B) forms, as well as at the docking surface of RC (C). The color code in units of k_BT for the electrostatic potential is as follows: +1, blue; 0, green; −1, red. The positions of heme and key charged residues are labeled.

subdividing the interface into a hydrophobic short-range interaction domain surrounded by an electrostatic long-range interaction domain as suggested by Tetreault et al.[9,10] On the cyt c_2 surface the short range interaction domain (central circle around the heme) is comprised mainly of hydrophobic and small polar residues. The small polar residues are either in direct contact or make contacts through bridging water molecules with the RC. The portion of the periplasmic surface of the RC that contacts the residues and water molecules in the short range interaction domain is omitted for clarity. As cyt c_2 is a globular protein docking to the relatively flat RC surface, only few residues contribute to the observed VDW contacts even at the point of optimal contact. This feature results in a docking interface with a small surface area, which is comparable to the interface in the cyt c−cyt c peroxidase complex exhibiting with 1170 Å^2 the smallest protein−protein complex interface studied so far.[20,40] As shown in Figure 2, the long range interaction domain is comprised of positively charged residues on the cyt c_2 surface and establishes functionally important long range electrostatic interactions with corresponding negatively charged residues on the RC surface. This charged outer region is highly solvated.

Average distances and standard deviations for individual RC−cyt c_2 interaction pairs from the last 2 ns of equilibration are compared in Table 1 to their values from the X-ray structure.[1] As expected, the largest variations are observed in the long-range electrostatic interaction domain. Using backbone harmonic constraints on the RC and cyt c_2 (in order to prevent dissociation of the cyt c_2 from the RC) Miyashita et al.[18] studied the dynamical effects at the RC−cyt c_2 interface by classical reorganizational energy sampling over a MD trajectory. Individual protein and solvent contributions to the reorganization energy were calculated in order to assess the fluctuations at the RC−cyt c_2 docking interface. The higher the contribution of individual docking surface residues and water to the reorganizational energy the higher the fluctuations. The results[18] indicate large contributions to the classical reorganizational energy from water and charged residues such as Lys and Asp on the docking surfaces of RC and cyt c_2, respectively, and small contributions from hydrophobic residues. As neither RC nor cyt c_2 is constrained in our simulations, the fluctuations observed arise through the combined movements of water and side chains as well as the overall motion of the proteins.

The two redox states of the RC−cyt c_2 system are distinguished by two different charge sets used for the heme prosthetic group. The charges developed for the cyt c_2^{ox} and cyt c_2^{red} forms are discussed in detail in ref 2. The simulated systems with the RC special pair in the neutral ground state and cyt c_2 in either the reduced or oxidized state resemble the RC−cyt c_2 systems employed for measurements of electron-transfer kinetics.[1,9] Figure 3 shows the electrostatic potential near the docking surfaces for RC and of cyt c_2^{red} and cyt c_2^{ox}. The location of charged residues shown by mutational studies[9,10] to be of major importance for docking are marked. It can be seen in Figure 3 that cyt c_2^{ox} has a slightly stronger positive potential on the docking surface compared to cyt c_2^{red}. The larger positive potential suggests that cyt c_2^{ox} might bind more tightly to the RC surface compared to cyt c_2^{red}. In a first binding study, Larson et al.[21] showed that horse heart cyt c in the presence of varying concentrations of detergent-solubilized RC from *Rb. sphaeroides*, reveals a 3.6-fold stronger binding affinity of oxidized cyt c to a single binding site. Native cyt c_2 exhibits much less of this tendency.[44] This result is surprising, as from a mechanistic point of view cyt c_2^{ox} should bind less tightly than cyt c_2^{red}. As will be discussed below stable water clusters establish themselves at the hydrophobic interface only for the reduced system. The water structure at the interface is highly dynamic for the oxidized system and could lead to the required undocking of cyt c_2^{ox}.

3.1.1. Short-Range Hydrophobic Domain. The main function of the short-range hydrophobic docking domain is to transfer electrons from cyt c_2 to the RC. The electron jumps from the exposed heme edge atom through the side chains of TyrL162, LeuM191, and ValM192 to the special pair inside the RC.[17,18] An apolar environment that does not permit indiscriminate electron transfer across space promotes optimal rates for directed electron transfer.[16] This is achieved through the short-range hydrophobic interaction domain as the residues form very tight VDW contacts connecting each other; this nonfluctuating hydrophobic tunneling domain guarantees optimal tunneling rates.[16−18]

As can be seen in Table 1 residue contacts establishing electron-transfer pathways are stable over the whole equilibration trajectory of 4 ns. The standard deviation is as low as 0.2 Å for the TyrL162:C_δ−Heme:CBC interaction pairs and not higher than 1.0 Å for VDW and hydrogen bond interaction pairs in both redox forms. The hydrophobic residue pairs with large standard deviations are all on the edge of the hydrophobic docking interface. TyrL162, which is suggested to be a key

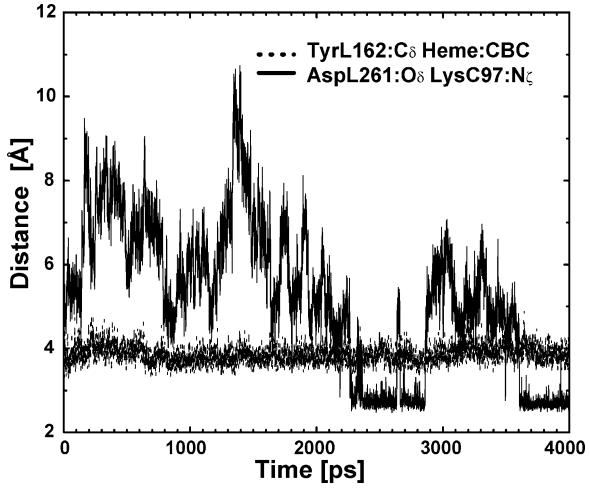

Figure 4. Stability of the hydrophobic and electrostatic docking domains during the course of 4 ns equilibration shown for two residue pairs. The TyrL162:C_δ−Heme:CBC contact exhibits weak fluctuations whereas AspL261:O_δ−LysC97:N_ζ exhibits strong fluctuations. The behavior of all RC−cyt c_2 residue pairs is summarized in Table 1.

residue for electron transfer[14,15] was mutated by Farchaus et al.[14,15] to Ser or Gly and most recently by Gong et al. to Ala.[17] Both groups observed approximately 100-fold decreases in electron-transfer rates. In addition, TyrL162 has been found to contribute very little to the reorganization energy.[18] Only one hydrogen bond (Gln *L*258:N_ϵ−LysC99:O) of the three observed interprotein hydrogen bonds in the X-ray structure was found to be stable over the course of our MD simulation.

3.1.2. Long-Range Interaction Domain. The charged residues contributing to the long-range interaction domain due to electrostatic forces exhibit large deviations from their initial conformation in the X-ray structure.[1] The standard deviation for all cyt c_2 interaction pairs involving Lys is always higher than 0.6 Å and is as high as 2.5 Å for the AspM184:O_δ − LysC97:N_ζ interaction pair in the RC−cyt c_2^{red} complex. Figure 4 shows the difference between the dynamically stable hydrophobic and the strongly fluctuating electrostatic domains for two representative RC−cyt c_2 interaction pairs, TyrL162:C_δ − Heme:CBC and AspL261:O_δ − LysC97:N_ζ. The distance between atoms AspL261:O_δ and LysC97:N_ζ varies from as large as 11 Å to as little as 2.5 Å. In the crystal structure no salt-bridges between these oppositely charged residues have been observed.[1] In contrast, our MD simulation exhibits the formation of a transient salt-bridge between these residues during the course of 4 ns. The salt-bridge fluctuates in and out during the last 2 ns of the simulation. Double mutational studies of *Rb. sphaeroides* RC and the homologous *Rb. capsulatus* cyt c_2 [10] revealed strong interactions between LysC99 and AspM184/GluM95 and between LysC54 and AspL261/AspL257. *Rb. sphaeroides* LysC97, located between both negatively charged RC clusters, most likely plays an important role in steering cyt c_2 toward its final docking position on the RC. As pointed out by Tetreault et al.,[9,10] specific interactions between oppositely charged RC−cyt c_2 residue pairs nucleate short-range hydrophobic contacts, but association must be weak as the complexes need to dissociate rapidly after electron transfer has occurred. The formation of transient salt-bridges supports this view as it allows long-range recognition of the complexes with weak association.

3.1.3. Interface Residues and Water. The water molecules shown in the top-down view of cyt c_2 in Figure 5 establish VDW as well as hydrogen bond contacts across the RC−cyt c_2 interface. The water molecules forming specific hydrogen bond interactions between RC and cyt c_2 are termed bridging water molecules[1] (WAT1, WAT2, WAT5, WAT10, WAT12, WAT13, and WAT20). In addition, there are two water molecules that contribute to VDW contacts between heme and RC (WAT3, WAT7). These water molecules are also identified in the X-ray structure. Accessibility of the docking interface to bulk water can be analyzed by monitoring the water molecules populating this region over the course of the simulations. Figure 5 shows the position of initial and final interface water molecules both at the beginning and at the end of the 4 ns MD simulation. The interface water, including bridging water molecules, is almost completely exchanged by bulk water after 4 ns of equilibration. Only three bridging water molecules are still on the cyt c_2^{red} surface at the end of the equilibration; even these water

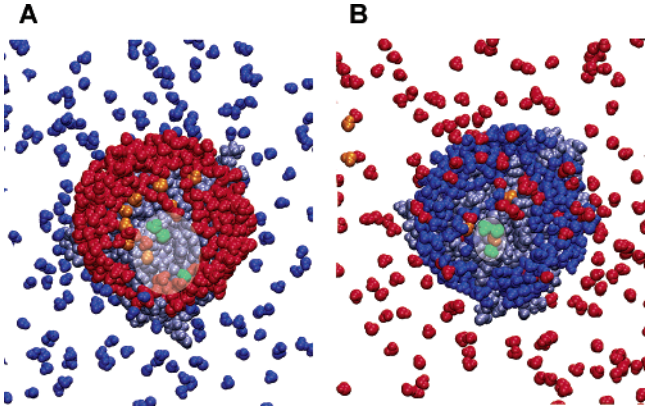

Figure 5. Top down view on the reduced cyt c_2 surface at the beginning (A) and end (B) of the 4 ns equilibration. Water molecules are colored based on their initial position. Bridging water molecules involved in hydrogen bonds and VDW contacts are colored in orange; single-file water molecules are colored in green. All other interface water molecules defined as water molecules within 20 Å of the central heme edge atom CBC are colored in red. The bulk water molecules are colored in blue. Almost all initial interface water molecules (red) get replaced by bulk water molecules (blue), and almost all bridging water molecules (orange) get exchanged. Three water molecules (green) and one bridging water molecule establish a stable hydrogen bonded single-file during the course of equilibration; these water molecules are located in the highlighted disks in part B. The hydrophobic domain is located in the disk highlighted in part A.

TABLE 2: Number of Water−Water Contacts and Residence Times for the Bridging Water Molecules

	water neighbors	bulk water neighbors	residence time (ns)
	Reduced System		
Wat1	0	0	>4.0
Wat2	3	2	1.0
Wat3	5	5	<0.1
Wat5	3	3	0.6
Wat7	1	1	>4.0
Wat10	3	3	<0.1
Wat12	3	3	<0.1
Wat13	2	2	0.4
Wat20	2	2	<0.1
	Oxidized System		
Wat1	0	0	>4.0
Wat2	2	2	>4.0
Wat3	1	0	2.7
Wat5	1	1	1.0
Wat7	2	1	3.4
Wat10	5	5	<0.1
Wat12	3	3	0.2
Wat13	5	5	<0.1
Wat20	3	2	0.2

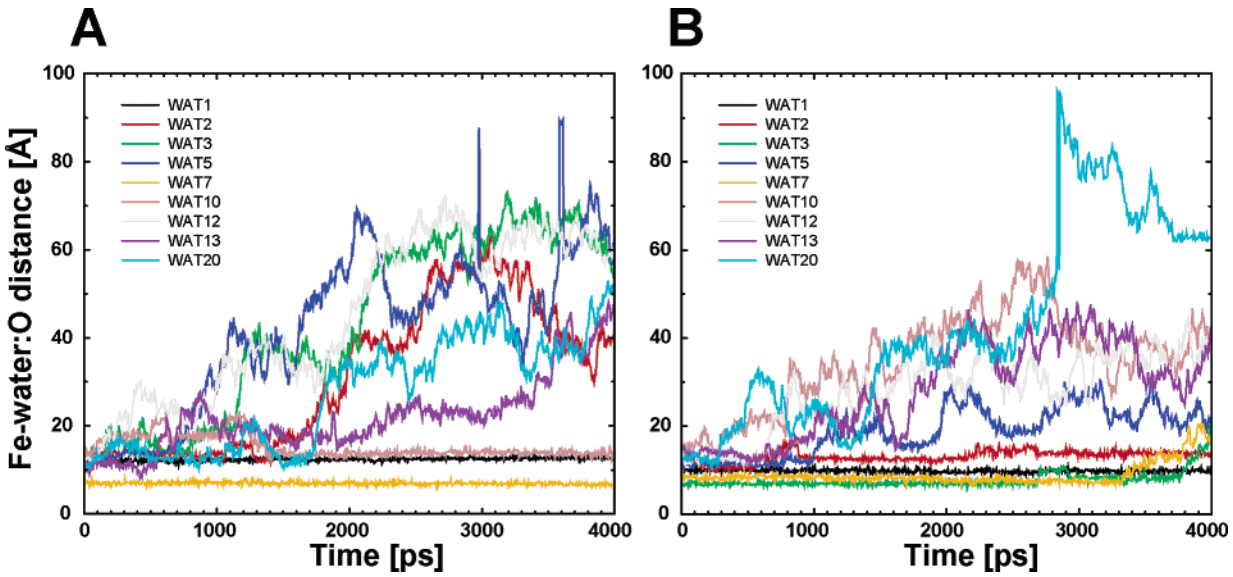

Figure 6. Exchange of bridging water with bulk in the reduced (A) and oxidized (B) systems. Shown is the distance between the heme iron and the oxygen of the individual water molecules used to monitor the residence of water molecules over the course of 4 ns equilibration. The numeric values of the residence times are given in Table 2.

molecules have relocated themselves along the surface within a few Ångströms. Table 2 shows the number of water−water contacts and the residence times for the bridging water molecules. With the exception of Wat1, all bridging water molecules are in contact with one to five water molecules within 3 Å. These neighboring water molecules can be either contacting bridging water molecules or bulk water molecules. A water molecule is considered as bulk water when it exhibits at least three hydrogen bond contacts to neighboring water molecules. Bridging water molecules exchange more rapidly when they are in direct contact with bulk water. Henchman and McCammon[41] have recently studied the residence time of water molecules as a function of their position in proteins. The calculated residence times range from 10^1 to 10^4 ps depending on the number of protein−water hydrogen bonds and how tightly they are buried inside the protein.[41] This more extensive study is in good agreement with our observations for the bridging water molecules as shown in Table 2. Only Wat1, which is buried inside a hydrophobic pocket and has three stable hydrogen bonds to the surrounding protein residues LeuM191:O, GlnC14:O, and ThrC17:O_γ [1] is not exchanged in either the reduced or the oxidized system. All other bridging water molecules exhibit residence times described by Henchman and McCammon,[41] which vary greatly in our two independent simulations. As we started to measure the residence times of the bridging water molecules after 0.5 ns preequilibration of water and lipids, we were unable to resolve the residence times in the ps time range.

The trajectories of the bridging water molecules are depicted in Figure 6. The distance between the heme iron and oxygen of individual water molecules shown in Figure 6 and Table 2 was measured from trajectory data. It can be seen that in both redox forms some water molecules are already exchanging at the beginning of the 4 ns equilibration phase, others remain at their initial position until the end of the equilibration, while some are stuck for several ns at the interface before they are finally exchanged. Our measurement reveals the overall dynamics, but cannot resolve relocations by a few Ångström along the surface.

We have found also that the orientation of bound interface water molecules depends on their position at the interface. As

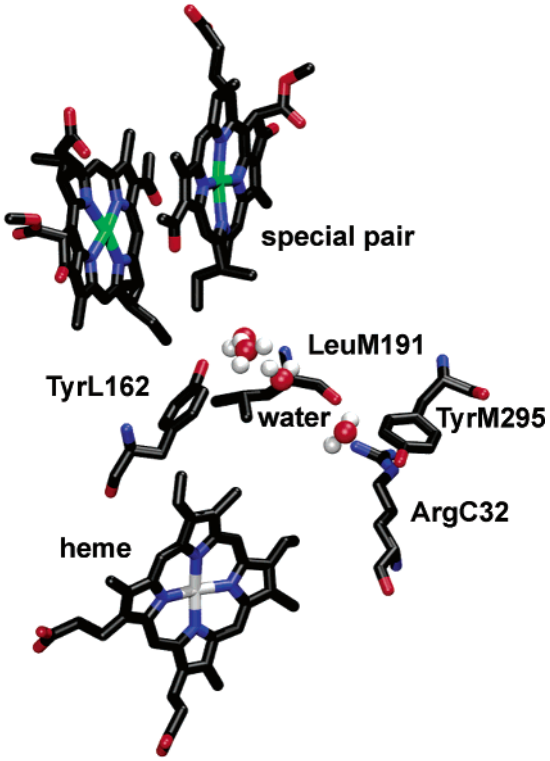

Figure 7. Four single-file water molecules within 4 Å of heme and the special pair. These water molecules connect ArgC32 and TyrM295, involved in a cation−π interaction, to electron-transfer residues TyrL162 and LeuM191. To simplify the view, residues ThrC17 and AsnM195 within 2.9 and 3.5 Å, respectively, of the single file water molecules are omitted.

a measure for the orientation, the dipole moment of individual water molecules has been determined as described in refs 42 and 43. The quantity monitored is cos $\alpha(\mu)$, where $\alpha(\mu)$ is the angle of the dipole moment μ relative to the z-axis. In contrast to bulk water, which possesses fast translational and rotational degrees of freedom, the interface water remains fixed as long as its molecules are trapped inside the interface.

3.1.4. Structural Water near the Cation—π Interaction Pair. The only major redox-dependent interaction between the

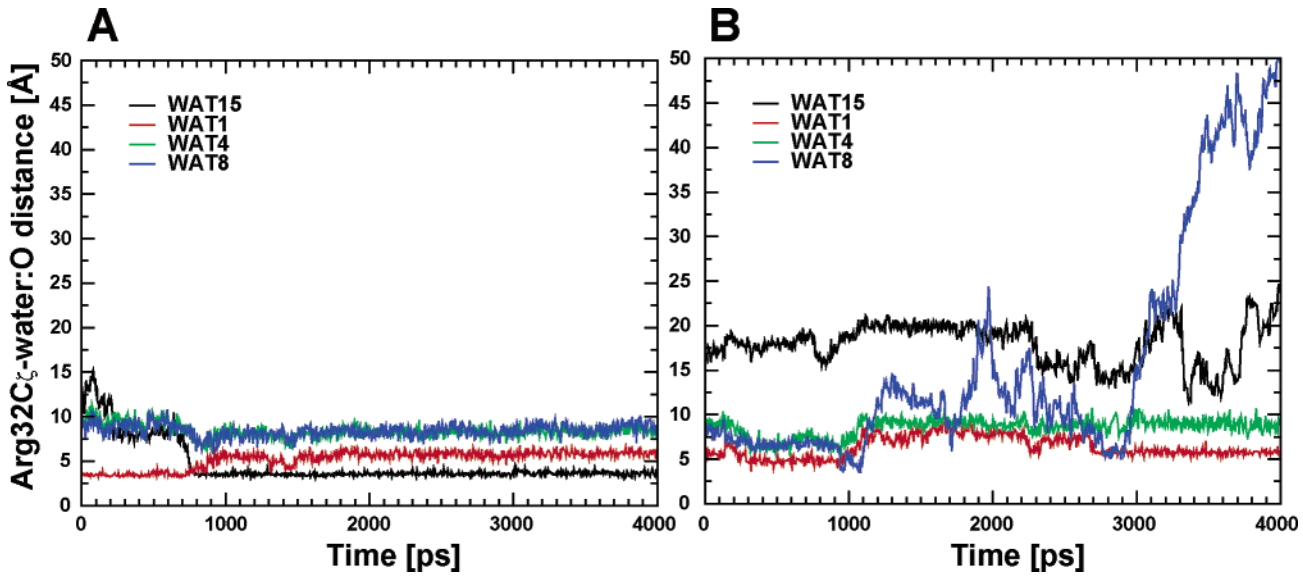

Figure 8. Dynamics of the single file water molecules. In the reduced system (A), four water molecules establish during the first ns of equilibration single-file hydrogen bonds with each other. This proposed electron-transfer hardwire is stable and not exchanged until the end of 4 ns equilibration. In the oxidized system (B), the four water molecules exhibit much larger movement at the interface and eventually exchange in a manner similar to the bridging water molecules in Figure 6.

simulated cyt c_2 and the RC was found in close proximity to the cation$-\pi$ interaction pair formed through direct contact between a charged cyt c_2 residue (ArgC32) and an aromatic RC residue (TyrM295). As shown in Figures 2 and 5, four water molecules (WAT15, WAT1, WAT4, and WAT8) form a hydrogen-bonded single file structure in the simulated RC$-$cyt c_2^{red} system. In Figure 7, the four single-file water molecules are shown to be located in a hydrophobic pocket close to the photosynthetic pigments connecting ArgC32 to the RC residues TyrL162 and LeuM191, which are important for electron transfer.[14,15,18]

The pocket is lined by ArgC32, ThrC17, LeuM191, AsnM195, and TyrL162, and the edge of the RC special pair near the CBC atoms. As shown in Figure 8, this water-mediated electron-transfer hardwire establishes itself only in the reduced system. In contrast to the exchanged bridging water molecules described in the previous section, these four water molecules diffuse into the interface during the first ns of equilibration, reorient themselves and establish an electron-transfer hardwire which is stable and not exchanged during the 4 ns equilibration. The only bridging water already found in the RC$-$cyt c_2 X-ray structure close to its final position is Wat1 which relocates itself by about 1 Å in order to make space for the three water molecules which move in shortly before the relocation takes place. In the X-ray structure, Wat4 and Wat8 are located in a hydrophobic RC pocket within 3 to 4 Å of TyrL162 and the RC special pair edge. Wat15 is initially located on the cyt c_2 surface. As shown in Figure 8a, Wat4 and Wat8 as well as Wat15 move several Å during the first ns in order to establish a stable single-file hydrogen bond structure connecting cyt c_2 to the RC. In particular, the water molecules Wat1, Wat4, and Wat8, which are in VDW contact with interfacial electron transferring residues, namely TyrL162 and LeuM191, never break the hydrogen bond contact with their respective water molecule partners. Wat15 hydrogen bonded to ArgC32 forms only temporarily a hydrogen bond to Wat1, but it is always connected via a hydrogen bond to ArgC32 during the course of our 4 ns equilibration. Miyashita et al.[18] have described in their simulations the following favorable pathway involving a single water molecule: Heme:CBC → water:O → AsnM187: O_δ → special pair:CMC. The water molecule in this respective structure is located close to TyrL162 and provides an alternative electron-transfer pathway at the interface.

In our simulations, a corresponding water molecule is also located in contact with the Heme:CBC, but it moves in from the bulk and is often exchanged.

As shown in Figure 8b, the oxidized form exhibits a different behavior around the cation$-\pi$ interaction pair. The four water molecules never form a single-file and exhibit essentially the same behavior as the other bridging water molecules. Wat1 and Wat4, which are trapped inside a hydrophobic binding pocket, close to the cation$-\pi$ pair, constantly relocate themselves inside the pocket but are not exchanged. In contrast, Wat8 and Wat15, initially bound to the RC and cyt c_2, respectively, are exchanged with the bulk during the course of the 4 ns equilibration. The dynamic behavior of water inside the hydrophobic pocket of the RC$-$cyt c_2^{ox} complex is demonstrated in a movie provided as Supporting Information. Water molecules move inside the pocket, get trapped, and move out, depending on the surrounding protein topology and their connection to bulk water. None of the water molecules forms stable hydrogen bonds to adjacent water molecules. In general, the water molecules at the interface of RC$-$cyt c_2^{ox} exhibit more fluctuations than for RC$-$cyt c_2^{red}.

The area around the cation$-\pi$ interaction pair is the only location where conformational changes on the RC due to the docking of cyt c_2 are observed in both RC and cyt c_2.[1] The aromatic ring of TyrM295 moves approximately 2 Å toward ArgC32 when comparing the RC$-$cyt c_2 complex to undocked RC structures. The single-file water molecules can enhance observed electron transfer across the interface.[16,18] There is a possibility that the cation$-\pi$ interaction is a water-mediated redox switch that establishes a tightly bound interface favorable for electron-transfer in the reduced form. After cyt c_2 oxidation, this temporary connection could be easily destroyed by relocation of one or two water molecules in the pathway leading to facilitated undocking of cyt c_2. As shown in Figure 3, a change in the charge state of the heme prosthetic group results in a change of electrostatic potential on the cyt c_2 docking surface far away from the central heme.[2] Our simulations suggest that

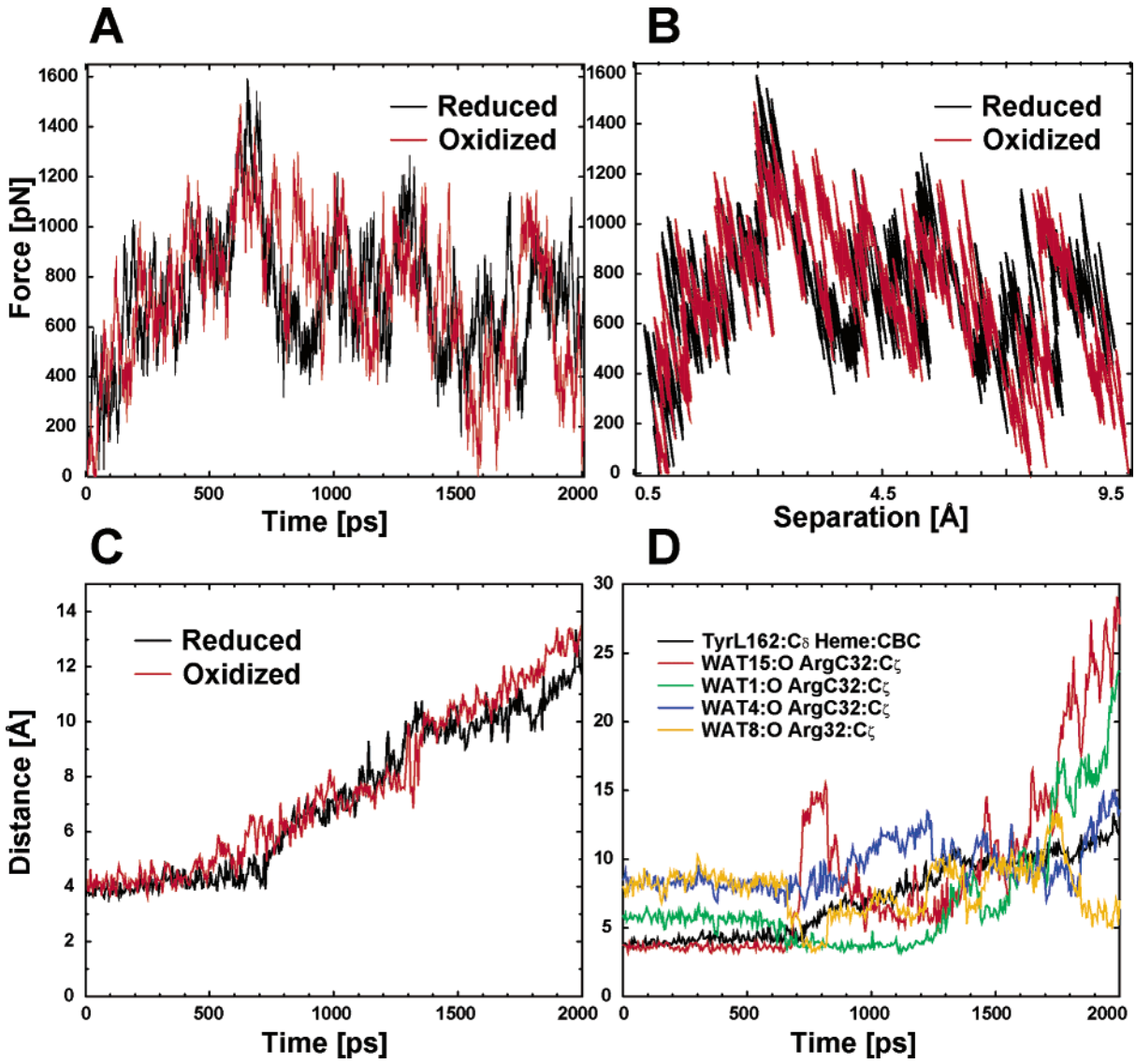

Figure 9. Analysis of SMD runs: (A) force vs time; (B) force vs separation; (C) evolution of the Tyr162:C_δ−Heme:CBC contact compared for reduced (black) and oxidized (red) systems; (D) single-file water molecules located in the hydrophobic pocket close to the cation−π interaction pair of the reduced system compared to the Tyr162-C_δ−Heme:CBC residue pair.

this charge change could be sensed by water molecules inside a hydrophobic pocket at the edge of the RC−cyt c_2 docking interface.

3.2. Probing RC—cyt c_2 Docking by Means of SMD. Constant velocity SMD runs for both redox forms revealed that the interface residues establishing VDW contacts between RC and cyt c_2 are of major importance for the stability of the complexes.

After 2 ns equilibration both cyt c_2^{red} and cyt c_2^{ox} were pulled 10 Å away from the RC by applying an external force on all cyt c_2 backbone atoms. The force peaks around 600 ps shown in Figure 9 correspond to the breakage of the VDW docking interface. The maximum breaking force required is slightly higher for cyt c_2^{red} (1600 pN) than for cyt c_2^{ox} (1500 pN). The force curves are within typical variations expected in SMD simulations, and no conclusive statements can be made at this moment about differences in undocking behavior between the reduced and oxidized systems.

As shown in Figure 9c, the breakage of the VDW interface was monitored by measuring the distance between the atoms TyrL162:C_δ and Heme:CBC, the most stable RC−cyt c_2 residue pair. One can discern that the TyrL162-heme interaction is broken in the oxidized system 100 ps earlier than in the reduced system. The final RC−cyt c_2 separation is approximately 0.5 Å larger for the oxidized system compared to the reduced system. The lower required force and larger separation for the oxidized system is consistent with the data shown in Table 1 exhibiting fluctuations of the VDW docking interface complex during the last 2 ns of equilibration, that are stronger for the RC−cyt c_2^{ox} than for the RC−cyt c_2^{red} complex. During the separation of RC and cyt c_2, the single file of four water molecules described above continues to establish stable hydrogen-bonds in the reduced system until the hydrophobic interface is broken as shown in Figure 9d. The hydrogen bonds break at the same time as the TyrL162−heme VDW contact disrupts. After 600 ps, WAT15 moves out rapidly and the hydrophobic contact region becomes accessible to bulk water molecules. At this point, the other three single-file water molecules form transient hydrogen bonds with bulk water and dislocate from their initial positions.

After the hydrophobic interface is broken the force required to pull the complexes apart is still fairly high and fluctuates between 0 and 1200 pN until the end of the 2 ns SMD runs. The required force is significantly larger than the force that

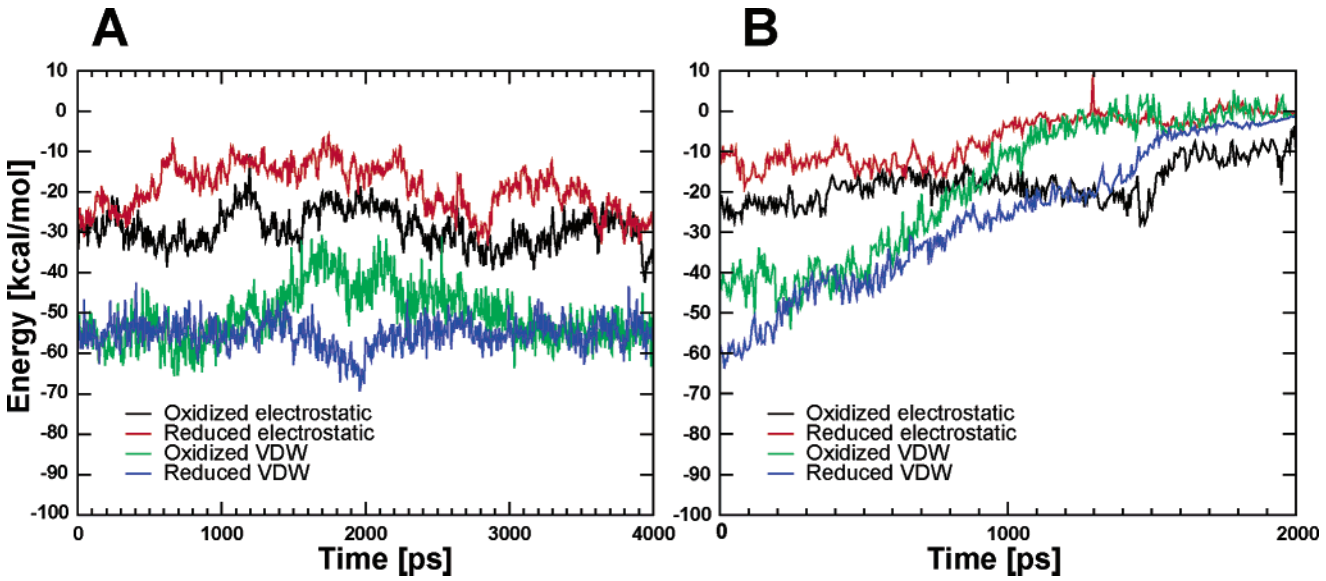

Figure 10. Interaction energies of docking during equilibration (A) and of 2 ns SMD simulation (B). The VDW energy contribution is energetically more favorable compared to the electrostatic energy contribution until the hydrophobic interface is broken.

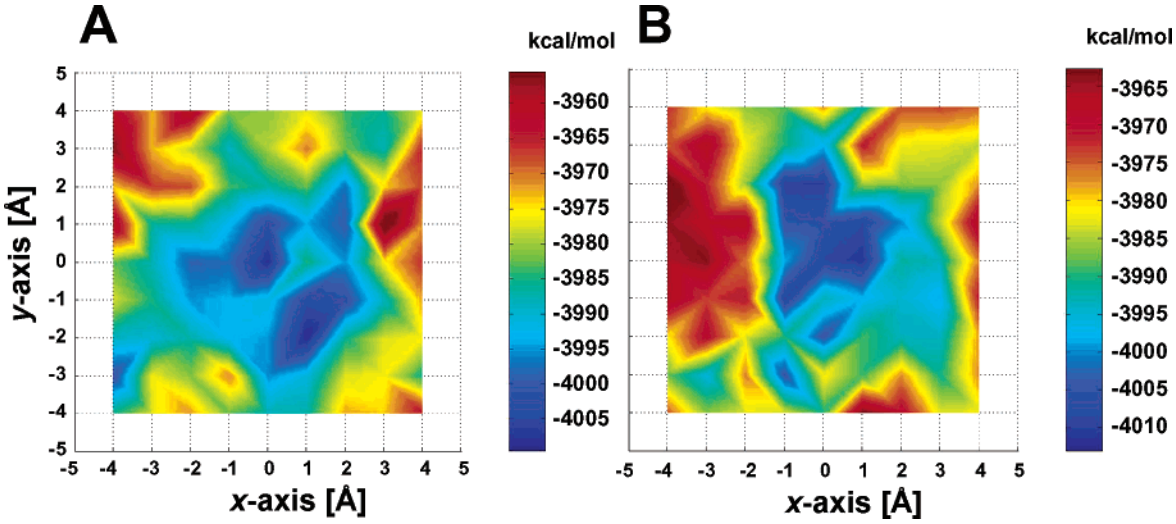

Figure 11. Cyt c_2 movement along the RC surface for the reduced (A) and oxidized system (B). Both redox systems exhibit a broad VDW minimum extending more than 2 Å in *X* and *Y* directions from the initial energy minimized RC−cyt c_2 docking position at [0,0].

would be needed to pull cyt c_2 through water (assuming a spherical shape of radius $a = 20$ Å and a pulling speed s of 0.01 Å/ps for cyt c_2, the Stoke force F_{fric} can be calculated using a friction coefficient $\eta = 0.891 \times 10^{-3}$ kg/ms and Stoke's formula $F_{fric} = 6\pi\eta as$, yielding a F_{fric} value as low as 35 pN). Cyt c_2 initially interacts with the RC by the electrostatic contacts observed during the course of equilibration. Force is required to disrupt these weak electrostatic contacts. For both the oxidized and the reduced complexes, the involved charged residues establish new electrostatic contacts as cyt c_2 is moved away from the RC surface. The Lys side chains on cyt c_2 extend toward the negatively charged residue clusters on the RC during the course of 2 ns SMD. In the RC−cyt c_2^{ox} complex, LysC97 and AspL261 are in salt-bridge distance at the beginning of the SMD simulations. During the simulation this transient salt-bridge becomes even stronger as RC and cyt c_2^{ox} are pulled apart. The LysC97−AspL261 salt-bridge persists until $t = 1.1$ ns. Subsequently, the weak LysC99−AspL257 interaction in close proximity becomes disrupted and LysC97 establishes two stable salt-bridges with two negatively charged RC residues AspL261 and AspL257. This very strong electrostatic interaction lasts until $t = 1.7$ ns and is replaced then by weak electrostatic interactions of LysC97 with AspL257. In the RC−cyt c_2^{red} complex, there arise only weak electrostatic interactions during the course of the 2 ns SMD simulation. Significant electrostatic interactions are still present even after the RC and cyt c_2^{ox} have been pulled 10 Å apart, as can be recognized from the movie provided as Supporting Information.

3.3 Energy Landscape of Docking. Figure 10a shows the individual RC−cyt c_2 interaction energy contributions during the course of equilibration. In the unperturbed complex where the two proteins are close to each other, the VDW contribution for the interaction energy is larger than the electrostatic contribution. To compare both energy contributions, the electrostatic energy contribution was scaled by a dielectric factor of 10. This value was chosen to account for the dielectric properties of water at the RC−cyt c_2 docking interface as suggested by Miyashita et al.[25] The VDW interaction energy is slightly lower for the reduced system than for the oxidized one indicating a closer fit between the two proteins in the reduced system, which is consistent with its more stable configuration. In contrast, the electrostatic interaction energy is lower for the

RC−cyt c_2^{ox} system due to an additional charge of $+1e$ in the oxidized heme group[2] favorably interacting with the negative surface of the RC. This positive charge increase will result in stronger Coulombic attraction for the oxidized RC−cyt c_2^{ox} complex.

Figure 10b shows the VDW and electrostatic contributions to the RC−cyt c_2 interaction energy during the course of our 2 ns SMD simulations. The forced undocking was started from conformations occurring after 2 ns of equilibration in which cyt c_2^{ox} had formed transient salt-bridges to the RC with LysC97 as described above. In the case of cyt c_2^{red} there was no initial salt-bridge after 2 ns of equilibration. A decrease of the VDW interaction energy can be observed after the hydrophobic interface is broken at $t = 600$ ps. The fluctuations of the electrostatic energy contribution can be explained through the continued electrostatic interactions between charged surface groups. During the last 500 ps of the SMD run, the electrostatic energy contribution becomes even larger for the RC−cyt c_2^{ox} system. This stronger electrostatic interaction is due to the formation of multiple salt-bridges with LysC97 described above. For cyt c_2^{red}, transient salt-bridges were not formed in the initial phase of the SMD simulation. Therefore, the electrostatic interaction monotonically decreases as the two proteins are separated. As the peaks of VDW and scaled electrostatic interaction energies differ from each other by not more than 50 kcal/mol there must be a balance between these two energy contributions in native cyt c_2 docking. The number of Lys residues on the cyt *c* docking surface varies from organism to organism in contrast to the residues forming the connection to the heme prosthetic group, which are conserved in all three domains of life.[11,12] This feature could explain the strong differences in binding kinetics for horse heart cyt *c* to photosynthetic RC compared to native *Rb. sphaeroides* cyt c_2 binding.[21] Horse heart cyt *c* has an overall charge of $+7$ *e* in the reduced state compared to *Rb. sphaeroides* cyt c_2 with an overall charge of -2 *e*.

3.4. Two-Dimensional VDW Docking Surface of cyt c_2. Figure 11 shows the VDW energy surface experienced when cyt c_2 is moved rigidly along the RC surface. Both redox forms exhibit a broad VDW minimum extending more than 2 Å in the *x* and *y* directions from the initially minimized RC−cyt c_2 docking position at [0,0]. This docking minimum in both redox forms is close to the position observed in the X-ray structure.[1] The broad shallow VDW surface at around −4005 kcal/mol in the reduced form and around −4010 kcal/mol in the oxidized form would allow cyt c_2 to find its optimal docking position even in the case of imprecise docking. The steering toward a rough initial position could be accomplished by long-range electrostatic interactions which could be followed by more precise docking through VDW contacts. The inferred high mobility of cyt c_2 on the surface of the RC in the encounter complex is consistent with experimental studies indicating that, in the docking transition state, the two proteins may be shifted as much as 10 Å from what is observed in the crystal structure of the complex.[45]

In fact, during the course of 4 ns free equilibration of the RC−cyt c_2 system, the cyt c_2 shifts along the RC surface. Figure 12 shows the relative movements of RC and cyt c_2. In both redox forms, the cyt c_2 center of mass moves along the *xy*-coordinates by more than 3 Å to a new docking orientation. The movement along the *z*-axis is 2 Å larger for the oxidized form compared to the reduced form, but both redox forms finally move back to their initial orientation. We cannot resolve from our simulations if the docking orientation at the end of 4 ns equilibration is energetically more favorable compared to the initial configuration in the crystal structure; motional fluctuations are as large as 2 Å, and it is more likely that cyt c_2 moves within the boundaries of a broad shallow energy minimum. Miyashita et al.[25] found a similar broad energy minimum for the electrostatic interactions. As shown in Table 1, the RC−cyt c_2 hydrophobic interface is never broken during the course of 4 ns equilibration, but the RC−cyt c_2 electrostatic interaction domain fluctuates significantly. As determined by Miyashita et al.[25] the contribution of electrostatic interaction to the binding energy is close to zero and slightly unfavorable.

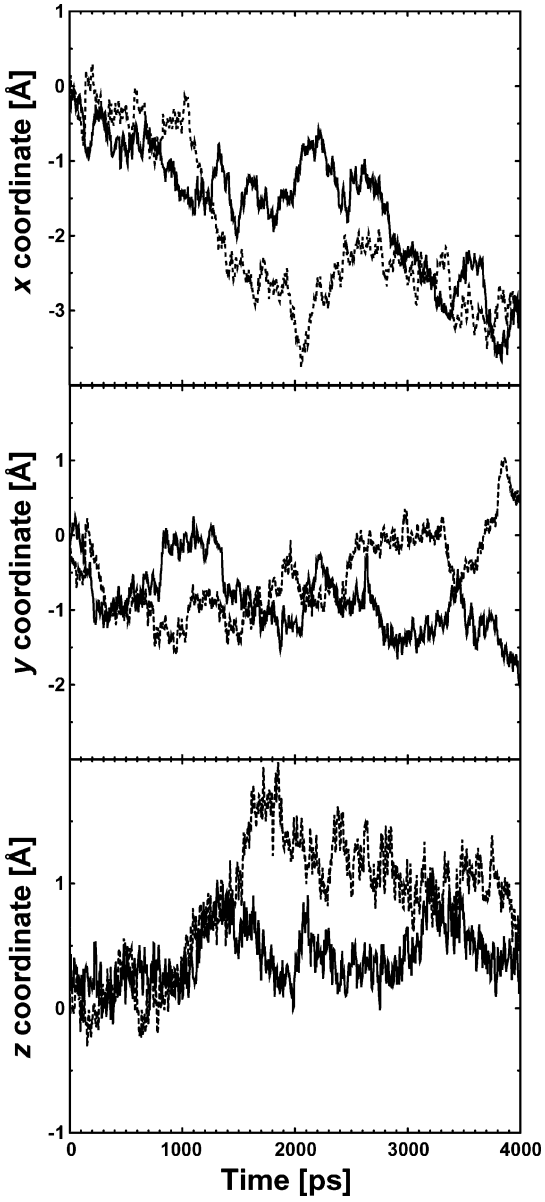

Figure 12. Relative center of mass displacement in three dimensions for the reduced (solid line) and oxidized (dashed line) systems. The large center of mass fluctuations can be best explained with a cyt c_2 wiggling motion at the energetically flat RC docking site.

4. Conclusions

Our studies of the RC−cyt c_2 encounter complex provide a dynamical picture of RC−cyt c_2 docking. In its overall dynamics the complex has been found to behave very similarly in both cyt c_2^{ox} and cyt c_2^{red}, exhibiting at the interface a stable hydrophobic tunneling domain and a dynamic electrostatic

steering domain. The differences between cyt c_2^{ox} and cyt c_2^{red} are subtle and involve the formation of structured water molecules in the reduced system. In contrast, cyt c_2^{ox} exhibits large fluctuations of interfacial water molecules. We suggest that single-file water molecules serve as a redox switch: water molecules could sense the change in electrostatic potential leading to facilitated undocking after oxidation.

SMD simulations that enforce undocking suggest that smaller forces are required to break the stable VDW contact in the oxidized system than in the reduced system. It also became evident in our study that VDW contacts are essential for transient RC−cyt c_2 docking. How cyt c_2 approaches its final RC docking position remains an open question. The most likely scenario is that cyt c_2 diffuses or slides along the membrane between its docking positions on the bc_1 complex and the RC. As it comes close to the RC periplasmic docking site, cyt c_2 experiences weak electrostatic forces guiding it close to its final docking position. The VDW energy surface around the docking position is shallow such that cyt c_2 can slide easily into a docking position optimal for electron transfer.

Acknowledgment. This work was funded by National Science Foundation Grants MCB02-35144 and MCB02-34938 and the National Institutes of Health Grant P41-RR05969. The authors acknowledge computational time provided by the National Resources Allocation Committee Grant MCA935028.

Supporting Information Available: Movies showing (1) the dynamic behavior of water inside the hydrophobic pocket of the RC−cyt c_2^{ox} complex and (2) a 2 ns SMD simulation demonstrating that significant electrostatic interactions are still present even after the RC and cyt c_2^{ox} have been pulled 10 Å apart. This material is available free of charge via the Internet at http://pubs.acs.org.

References and Notes

(1) Axelrod, H. L.; Abresch, E. C.; Okamura, M. Y.; Yeh, A. P.; Rees, D. C.; Feher, G. *J. Mol. Biol.* **2002**, *319*, 501.
(2) Autenrieth, F.; Tajkhorshid, E.; Baudry, J.; Luthey-Schulten, Z. *J. Comput. Chem.* **2004**, *25*, 1613.
(3) Lange, C.; Hunte, C. *Proc. Natl. Acad. Sci. U.S.A.* **2002**, *99*, 2800.
(4) Hu, X.; Ritz, T.; Damjanović, A.; Autenrieth, F.; Schulten, K. *Q. Rev. Biophys.* **2002**, *35*, 1.
(5) Allen, J. P.; Feher, G.; Yeates, T. O.; Komiya, H.; Rees, D. C. *Proc. Natl. Acad. Sci. U.S.A.* **1987**, *84*, 6162.
(6) Adir, N.; Axelrod, H. L.; Beroza, P.; Isaacson, R. A.; Rongey, S. H.; Okamura, M. Y.; Feher, G. *Biochemistry* **1996**, *35*, 2535.
(7) Tiede, D. M.; Vashishta, A. C.; Gunner, M. R. *Biochemistry* **1993**, *32*, 4515.
(8) Lancaster, C. R. D.; Michel, H. *Structure* **1997**, *5*, 1339.
(9) Tetreault, M.; Rongey, S. H.; Feher, G.; Okamura, M. Y. *Biochemistry* **2001**, *40*, 8452.
(10) Tetreault, M.; Cusanovich, M.; Meyer, T.; Axelrod, H.; Okamura, M. Y. *Biochemistry* **2002**, *41*, 5807.
(11) Dickerson, R. E. *Nature* **1980**, *283*, 210.
(12) Berg, J.; Tymoczko, J.; Stryer, L. *Biochemistry*; W. H. Freeman and Company: San Francisco, CA, 2002.
(13) Deisenhofer, J.; Epp, O.; Miki, K.; Huber, R.; Michel, H. *Nature* **1985**, *318*, 618.
(14) Farchaus, J. W.; Wachtveitl, J.; Mathis, P.; Oesterhelt, D. *Biochemistry* **1993**, *32*, 10885.
(15) Farchaus, J. W.; Wachtveitl, J.; Mathis, P.; Oesterhelt, D. *Biochemistry* **1993**, *32*, 10894.
(16) Tezcan, F. A.; Crane, B. R.; Winkler, J. R.; Gray, H. B. *Proc. Natl. Acad. Sci. U.S.A.* **2001**, *98*, 5002.
(17) Gong, X. M.; Paddock, M. L.; Okamura, M. Y. *Biochemistry* **2003**, *42*, 14492.
(18) Miyashita, O.; Okamura, M. Y.; Onuchic, J. N. *J. Phys. Chem. B* **2003**, *107*, 1230.
(19) Holzapfel, W.; Finkele, U.; Kaiser, W.; Oesterhelt, D.; Scheer, H.; Stilz, H. U.; Zinth, W. *Proc. Natl. Acad. Sci. U.S.A.* **1990**, *87*, 5168.
(20) Pelletier, H.; Kraut, J. *Science* **1992**, *258*, 1748.
(21) Larson, J. W.; Wraight, C. A. *Biochemistry* **2000**, *39*, 14822.
(22) Izrailev, S.; Stepaniants, S.; Isralewitz, B.; Kosztin, D.; Lu, H.; Molnar, F.; Wriggers, W.; Schulten, K. In *Steered Molecular Dynamics*; Deuflhard, P., Hermans, J., Leimkuhler, B., Mark, A. E., Reich, S., Skeel, R. D.; Eds.; Computational Molecular Dynamics: Challenges, Methods, Ideas. Lecture Notes in Computational Science and Engineering 4; Springer-Verlag: Berlin, 1998; pp 39−65.
(23) Lu, H.; Isralewitz, B.; Krammer, A.; Vogel, V.; Schulten, K. *Biophys. J.* **1998**, *75*, 662.
(24) Isralewitz, B.; Gao, M.; Schulten, K. *Curr. Opin. Struct. Biol.* **2001**, *11*, 224.
(25) Miyashita, O.; Onuchic, J. N.; Okamura, M. Y. *Biochemistry* **2003**, *42*, 11651.
(26) InsightII, Molecular Simulations Inc. Technical report, Burlington, MA, 2000.
(27) Stowell, M. H. B.; McPhillips, T. M.; Rees, D. C.; Soltis, S. M.; Abresch, E.; Feher, G. *Science* **1997**, *276*, 812.
(28) Ducruix, A.; Reiss-Husson, F. *J. Mol. Biol.* **1987**, *20*, 419.
(29) Damjanović, A.; Kosztin, I.; Kleinekathöfer, U.; Schulten, K. *Phys. Rev. E* **2002**, *65*, 031919.
(30) Humphrey, W. F.; Dalke, A.; Schulten, K. *J. Mol. Graphics* **1996**, *14*, 33.
(31) Brooks, B. R.; Bruccoleri, R. E.; Olafson, B. D.; States, D. J.; Swaminathan, S.; Karplus, M. *J. Comput. Chem.* **1983**, *4*, 187.
(32) MacKerell, A. D.; Bashford, D.; Bellot, M.; Dunbrack, R. L., Jr.; Evansec, J. D.; Field, M. J.; Fisher, S.; Gao, J.; Guo, H.; Ha, S.; Joseph, D.; Kuchnir, L.; K, K. Kuczera; Lau, F. T. K.; Mattos, C.; Michnick, S.; Ngo, T.; Nguyen, D. T.; Prodhom, B.; Reiher, I. W. E.; Roux, B.; Schlenkrich, M.; Smith, J.; Stote, R.; Straub, J.; Watanabe, M.; Wiorkiewicz-Kuczera, J.; Yin, D.; Karplus, M. *J. Phys. Chem. B* **1998**, *102*, 3586.
(33) Jorgensen, W. L.; Chandrasekhar, J.; Madura, J. D.; Impey, R. W.; Klein, M. L. *J. Chem. Phys.* **1983**, *79*, 926.
(34) Kalé, L.; Skeel, R.; Bhandarkar, M.; Brunner, R.; Gursoy, A.; Krawetz, N.; Phillips, J.; Shinozaki, A.; Varadarajan, K.; Schulten, K. *J. Comput. Phys.* **1999**, *151*, 283.
(35) Grubmüller, H. Technical report, Theoretical Biophysics Group, Institute for Medical Optics, Ludwig-Maximilians University, Munich, 1996.
(36) Zhang, L.; Hermans, J. *Proteins Struct. Funct. Genet.* **1996**, *24*, 433.
(37) Darden, T.; York, D.; Pedersen, L. *J. Chem. Phys.* **1993**, *98*, 10089.
(38) Grubmüller, H.; Heller, H.; Windemuth, A.; Schulten, K. *Mol. Simu.* **1991**, *6*, 121.
(39) Bayas, M. V.; Schulten, K.; Leckband, D. *Biophys. J.* **2003**, *84*, 2223.
(40) Lo Conte, L.; Chothia, C.; Janin, J. *J. Mol. Biol.* **1999**, *285*, 2177.
(41) Henchman, R. H.; McCammon, J. A. *Protein Sci.* **2002**, *11*, 2080.
(42) Tajkhorshid, E.; Nollert, P.; Jensen, M. Ø.; Miercke, L. J. W.; O'Connell, J.; Stroud, R. M.; Schulten, K. *Science* **2002**, *296*, 525.
(43) Jensen, M. Ø.; Tajkhorshid, E.; Schulten, K. *Biophys. J.* **2003**, *85*, 2884.
(44) Wraight, C. Personal communication.
(45) Onuchic, J.; Okamura, M. Personal communication.